Journal of Applied Polymer Science

Influence of support layer and PDMS coating conditions on composite membrane performance for ethanol/water separation by pervaporation

Parimal V Naik, Roy Bernstein, Ivo F. J Vankelecom
Centre for Surface Chemistry and Catalysis, Faculty of Bioengineering Sciences, KU Leuven, Kasteelpark Arenberg 23, PO Box 2461, Leuven, 3001, Belgium
Correspondence to: I. F. J. Vankelecom (E-mail: ivo.vankelecom@biw.kuleuven.be)

ABSTRACT: A systematic study was performed on the combination of support properties and polydimethylsiloxane (PDMS) coating conditions for the lab-scale preparation of a defect-free, thin film composite membrane for organophilic pervaporation. Support layers having comparable surface porosities were prepared from three polymers with different chemical composition (PVDF, PSF, PI). Their exact role on the deposition of the PDMS coating (i.e., wetting and intrusion) and the final membrane performance (i.e., effect on mass transfer of the permeants) was studied. The crosslinking behavior of dilute PDMS solutions was studied by viscosity measurements to optimize the coating layer thickness, support intrusion and wetting. It was found essential to pre-crosslink the PDMS solution for a certain time prior to the coating. Dip time for coating the PDMS solution on the supports was varied by using automated dip coating machine. The performance of the synthesized membranes was tested in the separation of ethanol/water mixtures by pervaporation. Both flux and selectivity of the membranes were clearly influenced by the support layer. Resistance of the support layers increased by increasing the polymer concentration in the casting solutions of the supports. Increasing the dip time of the PDMS coating solution led to increased selectivity of the composite membranes. Scanning Electron Microscopy analysis of the composite membranes showed that this leads to a minor increase in the thickness of the PDMS top layer. Top layer thickness increased linearly with the square root of the dip time ($t^{0.5}$) at a constant withdrawal speed of the support. © 2016 Wiley Periodicals, Inc. J. Appl. Polym. Sci. **2016**, *133*, 43670.

KEYWORDS: films; membranes; separation techniques

Received 17 October 2015; accepted 21 March 2016
DOI: 10.1002/app.43670

INTRODUCTION

Owing to the emerging inadequacy of oil resources and the increase in their prices, it is assumed that fossil energy sources eventually need to be replaced gradually by renewable substrates. Biomass energy systems are one of the most immediate and important options available nowadays for sustainable development.[1] In this respect, fermentation is an attractive process for producing ethanol from renewable biomass.[1–4] One approach to improve the productivity of the ethanol fermentation is to continuously remove ethanol from the fermentation broth as it is produced, thus reducing the inhibitory effect of high ethanol concentrations on the yeast performance. This approach would also allow continuous fermentation to be conducted. The proposed techniques for ethanol recovery from fermentation broths currently include vacuum distillation,[5] solvent extraction,[6] gas stripping,[7] and membrane pervaporation.[8–10]

Pervaporation (PV) is a membrane separation process in which vacuum or sweep gas is applied at the downstream side of the membrane to create the driving force.[11] Membranes applied in pervaporation are composite membranes, consisting of a very thin, selective, top-layer, and a porous support layer. Ideally, the active layer should provide excellent flux and selectivity, while the support layer should exhibit mechanical stability and not interfere with the mass transport at all.

Several studies have demonstrated that the support layer can have significant effects on pervaporation.[12–33] Some studies focused on inorganic materials as support, for example, ceramic[31–33] while polyacrylonitrile (PAN) is one of the most common polymer supports used in pervaporation.[14,15] In the hydrophobic pervaporation of multicomponent mixtures, support materials should be hydrophobic to improve the fluxes and selectivities of the organic compounds,[16] Intrusion of PDMS in pre-treated polysulfone (PSF) and polyvinylidene fluoride (PVDF) support layers changed the normalized fluxes of the composite membrane, while the selectivity remained the same. It was also noted that without support pre-treatment (filling the pores with water), it was not possible to prevent the PDMS

intrusion into the support,[25] and that the separation performance was strongly related to the silicone rubber composition, that is, nature of the Si- substituents.[26] Asymmetric cross-linked polyimide (PI) supports were coated with a dense PDMS layer where the skin-layer prevented the intrusion of the PDMS solution into the pores.[17] In PDMS/PSF composite membranes, the evaporation time of the NMP-based solution PSF before immersion in the nonsolvent bath proved to influence the mass transfer in pervaporation.[27] PAN supports were found to be less suitable to coat PDMS top-layers due to their high surface roughness.[28] In addition, it was difficult to reduce the pore size of PAN membranes due to the poor solubility of PAN, preventing casting from concentrated solutions.[34] The rather poor mechanical strength of PAN also often led to leaks. Even though many types of PAN polymers and copolymers exist, it is thus not obvious to turn PAN into a good support material for PDMS-based pervaporation membranes.

Apart from the good quality of the support, it is essential to prepare an appropriate PDMS coating solution to obtain good quality composite membranes. In general, the viscosity of the PDMS solution should be sufficiently high to make a defect-free coating. For most types of PDMS, it is then necessary to pre-crosslink the coating solutions to achieve the appropriate viscosity.[35] When the coating solution is highly viscous, a thick PDMS layer is obtained, whereas pore intrusion and defects are obtained when not viscous enough.[36,37] It is thus desirable to have a solution with a relatively low PDMS concentration to have the layer thin enough, but with adequate viscosity to prevent pore intrusion and defect creation.

To coat at lab-scale PDMS solutions on porous supports, different methods such as film casting, spin coating, dip coating, or spray techniques have been reported.[38] In "dip-coating," the top layer is formed by immersing the substrate in an appropriate polymer solution.[39] Some studies have investigated the effects of PDMS coating conditions, such as concentration of coating solution, solvent type, and number of coatings on performance of the prepared composite membranes.[40,41] However, the effect of variation in dip time for coating the PDMS solution has not been reported so far.

In this study, PSF, PI, and PVDF will be screened as alternative polymeric supports for PAN. Rationale behind choosing these polymers to prepare supports was the difference in their chemical structure, hence surface tension and hydrophilicity: PVDF is hydrophobic, PSF has a moderate hydrophilicity and PI is relatively more hydrophilic than PSF.[42] They all thus have different functional groups to interact with the PDMS. All these polymers are easy to process, readily available, and possess good mechanical, thermal, and chemical properties. Moreover, it is generally easy to prepare asymmetric membranes by the phase inversion method from these materials.[43–48] Next, an appropriate combination of support and coating conditions was searched for at lab-scale to fabricate thin, defect-free composite PDMS membranes for pervaporation. Dip time of the support in the PDMS solution as well as pre-crosslinking of the PDMS solution were optimized to obtain a thin, defect-free coating solution using an automated dip coating machine.

Table I. Casting Solution and Nonsolvent Bath Composition

Polymer	Solvent	Concentration (wt %)	Nonsolvent
PSF	NMP	16, 18, 20	Distilled water
PI	DMF		
PVDF	DMF		

EXPERIMENTAL

Chemicals

Polysulfone (PSF, UDEL P-1835, Mw= 81000 g/mol, PDI= 3.6, and polyvinylidene fluoride (PVDF, Solef 6010, Mw= 320000, PDI = 2.1) were kindly supplied by Solvay (Belgium), Polyimide (PI, Matrimid® 9725, MW= 33000 g/mol, PDI = 2.0) was kindly provided by Huntsman (Switzerland). All polymers were dried in an oven overnight at 110 °C. Polydimethylsiloxane (PDMS, RTV-615, comprising two components A and B) was obtained from GE silicones (Belgium), *N*-methyl pyrrolidinone (NMP, 99%), and dimethylformamide (DMF, 99%), were obtained from Acros Organics. Ethanol (99.9%) and hexane (99%) were purchased from VWR. All solvents were used as received. The non-woven polypropylene/polyethylene fabric Novatexx 2471 was generously supplied by Freudenberg filtration technologies (Germany).

Support Synthesis

Asymmetric supports were prepared via the nonsolvent induced phase separation process. Casting solutions were prepared as presented in Table I by dissolving the polymers in respective solvents at room temperature. After dissolution, these casting solutions were kept undisturbed for at least 24 h to remove the air bubbles. The polymer solutions were then cast at a speed of 1.2 m/min on a PP/PE non-woven fabric using an automated casting knife (Braive Instruments, Belgium) set at a gap of 250 μm. To prevent excessive penetration of the polymer solution, the non-woven fabric was first impregnated with solvent and then wiped dry before coating. The resulting film was immediately immersed in the nonsolvent coagulation bath (de-ionized water) at room temperature for 10 min. Three replicate supports were cast from each solution. These membranes were stored in distilled water until use.

Support Porosity Determination

The porosity ε (%) for the standalone supports was calculated gravimetrically by eq. (1), as reported by Li *et al.*[49] It is defined as the volume of the pores divided by the total volume of the microporous membrane, determining the weight of liquid (ethanol) contained in the membrane pores.

$$\varepsilon = \frac{(m_1 - m_2)/\rho_E}{(m_1 - m_2)/\rho_E + m_2/\rho_P} \times 100\% \quad (1)$$

where m_1 is the weight of the wet support (g); m^2 is the weight of the dry support(g); ρ_E is the ethanol density (0.789 g/cm^3); and ρ_P is the polymer density (PSF = 1.24 g/cm^3, PI = 1.20 g/cm^3, PVDF = 1.78 g/cm^3).[50–52]

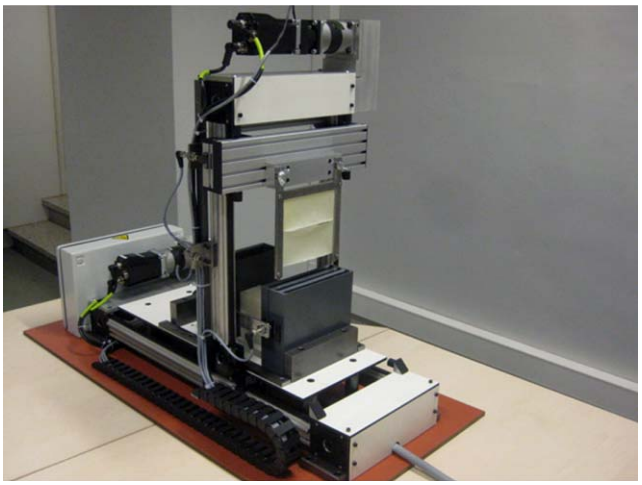

Figure 1. Automatic dip coating machine.[53] [Color figure can be viewed in the online issue, which is available at wileyonlinelibrary.com.]

Viscosity Measurement of PDMS Coating Solutions

Pre-crosslinking behavior of the PDMS solutions was studied as a function of reaction time by viscosity measurements performed on a stress- controlled rheometer (Anton Paar MCR501) with a cone-plate geometry and a solvent trap. PDMS solutions of three concentrations (5%, 10%, and 20 wt %) were prepared in *n*-hexane. Hundred mL of the solutions was stirred at 60 °C and 300 rpm for crosslinking in a 250 mL closed glass bottles to avoid solvent evaporation. The viscosity of each solution was measured each hour at a shear rate of 100 s^{-1} till it reached a viscosity of 100 mPa s.

Preparation of Composite Membranes by Dip Coating

PDMS composite membranes were prepared by coating a thin layer of PDMS onto the supports using an automated dip coating machine shown in Figure 1 (HTML, Belgium).[53] To avoid collapsing of the pores and intrusion of PDMS solution inside the pores, these supports were treated with different solvent exchange baths of ethanol, iso-propanol and finally hexane, prior to the coating. The PDMS coating solution was prepared by slightly modifying the procedure described by Wessling *et al.*[33] A 100 mL solution of 10 wt % PDMS (RTV615A:RTV615B = 10:1) in hexane was pre-cross-linked at 60 °C for 4 h with stirring at 300 rpm in a 250 mL closed glass bottle to avoid solvent evaporation and to have a sufficiently viscous solution. (The reason for using 10 wt % of PDMS coating solution is well-explained in the section 4.2). This solution was then coated on the supports by immersing them in the solution bath, all supports were pre-soaked in hexane before coating the PDMS solution. Dip time was varied from 1 to 4 min while a removal speed of 0.010 m/s was maintained. After coating, the membranes were kept at room temperature for 30 min to evaporate most of the hexane and then kept in the oven at 110 °C for 1 h to complete the crosslinking. All the composite membranes were prepared in a same way and stored in dust-free environment.

Pervaporation Setup

A cross-flow pervaporation module was used in the experiments, as represented in Figure 2. It consists of three circular stainless steel cells in series. Membranes were placed on the bottom plates and covered by a surface area reducer leaving an active membrane area of 0.001589 m^2. A feed pump was used to circulate the feed through the cells at a speed of 1 L/min to avoid concentration polarization, realizing a Reynolds number of 5780 for the system by using eq. (2).

$$Re = \frac{\rho \upsilon d_h}{\mu} \tag{2}$$

where, *Re* is the Reynolds number, ρ is the density of the fluid (kg/m^3), υ is the kinematic velocity (m^2/s), d_h is the hydraulic diameter of the pipe (m), and μ the dynamic viscosity of the fluid (Pa.s). The temperature was kept constant at 40 °C. During pervaporation, vacuum was applied on the permeate side and maintained constant (< 1 mbar) with the digital pressure gauge to ensure enough driving force throughout the separation

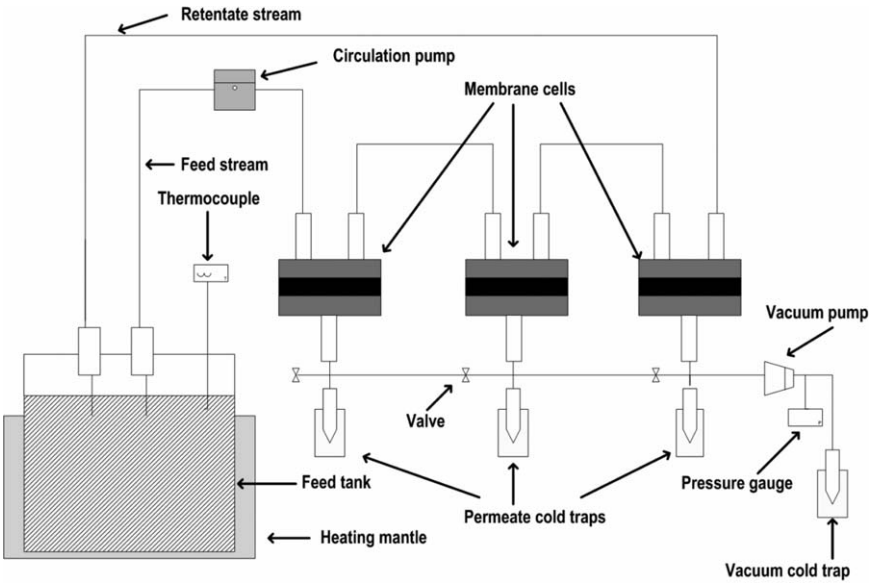

Figure 2. Pervaporation cross flow setup with three membrane cells in series.

process. To obtain constant flux, membranes were left to reach steady state for at least 12 h. Two samples were collected from each membrane after approximately 3 and 6 h. Each membrane type was prepared in duplicate. Two coupons were taken from each duplicate, thus leaving four samples to be tested per membrane composition. Experiments were carried out with ethanol/water mixtures, with alcohol concentration of 6 wt %. Obtained permeates were collected as a function of time in round bottom glass containers using liquid nitrogen in a dewar flask as a cooling trap. The concentration of ethanol in the permeate samples was determined using a refractometer (ATAGO RX-7000α). Normalized flux (J) was calculated by using eq. (3) by considering the PDMS top layer thickness as obtained from Scanning Electron Microscopy (SEM).

$$J = \frac{m}{A.t} \times \frac{\delta}{10} \tag{3}$$

with m, the mass of the sample (kg); A, the active membrane area (m^2); t, the collection time (h); δ, the thickness of the PDMS top layer (μm) and 10, the thickness normalization factor (μm). The enrichment factor of the membrane was calculated by eq. (4) as follows:

$$\beta = \frac{\left(\frac{x_A}{x_B}\right)_{\text{permeate}}}{\left(\frac{x_A}{x_B}\right)_{\text{feed}}} \tag{4}$$

where x is a weight fraction, A represents the preferential component (ethanol) and B stands for water.

To integrate membrane flux and separation factor, the pervaporation separation index (PSI) was calculated using eq. (5):

$$\text{PSI} = J \times (\beta - 1) \tag{5}$$

where J is expressed in kg m^{-2} h^{-1}.

CHARACTERIZATION

Pure Water Flux of Supports

To evaluate the porosity of the supports, pure water fluxes were measured by using a standard Amicon® cell[54] at room temperature. Three coupons were cut from each membrane strip and per coupon three samples were analyzed. Membrane permeance (Lp) was calculated (L/m^2.h.bar) using eq. (6) as follows:

$$L_p = \frac{V}{At\Delta P} \tag{6}$$

where V is the permeate volume (L), A is the membrane area (m^2), t is the time (h), and ΔP is the pressure difference (bar).

Scanning Electron Microscopy

Scanning electron microscopy (SEM) was used to take images of surface sections of the supports and composite membrane cross-sections (obtained by breaking membranes submerged in liquid nitrogen). Pictures were acquired at 10.0 kV on a Philips XL 30 FEG-SEM. Samples were mounted onto SEM sample holders and coated with a 1.5–2 nm thick gold layer to reduce sample charging under the electron beam.

Gas Permeation Measurements

Composite membranes were assessed by single gas (CO_2) permeation measurements to determine the thickness of the PDMS layer on top and inside the pores using high-throughput gas separation setup (HTGS).[53] The gas flux was measured by a constant volume auxiliary cylinder connected to an MKS Baratron pressure transducer (feed pressure of 5 bar and downstream pressure of 1 mbar). Initially, the line from collector to the HT-module was evacuated by a vacuum pump for almost 2 h to remove residual air and to equilibrate permeation through the membrane. The feed gas was purged into the system at a rate of 1 l/min. The upstream pressure was adjusted by a back-pressure regulator mounted on the purge line. To measure the gas permeability, the valve between the auxiliary cylinder and the vacuum pump was closed down. The permeate gas was thus allowed to expand in the auxiliary cylinder. CO_2 gas permeability of self-supporting PDMS membrane was determined as a reference.

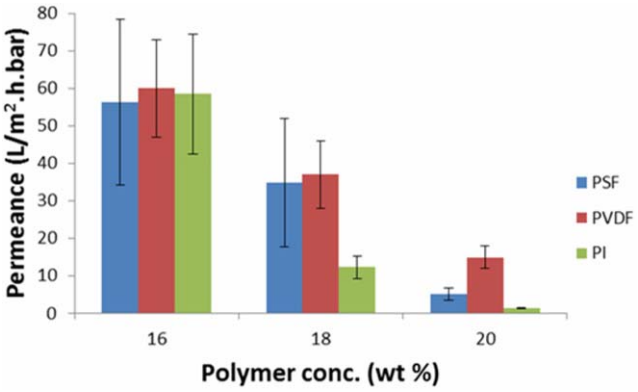

Figure 3. Pure water permeance of the supports as a function of polymer type and polymer concentration in the casting solution. [Color figure can be viewed in the online issue, which is available at wileyonlinelibrary.com.]

RESULTS AND DISCUSSION

Supports

From the three different chemistries that were selected, a set of supports was prepared first to obtain supports with comparable surface porosities for each chemistry. Pure water flux, bulk properties and pore morphologies of the supports were determined for three supports cast from solutions with different polymer concentrations for each chemistry.

Pure Water Fluxes of Supports. Pure water permeances of the supports prepared from the three different polymers and for each from three different casting solution concentrations, are shown in Figure 3. The values fall within the range of ultrafiltration (20–70 L/m^2.h.bar for supports prepared from 16 wt % and 18 wt % casting solutions) to nanofiltration (2–10 L/m^2 h bar for 20 wt %). PVDF supports show in general slightly higher permeances than PSF and PI supports when cast from solutions with the same polymer concentration, even though the standard deviations (mostly obtained from analysis of three permeate samples per coupon, using three coupons per membrane type cast in triple) are often rather large.

Support Porosity. The bulk porosities of the supports are shown in Figure 4. Porosity values fall within the range of 60 to 83%. PVDF membranes generally show a somewhat higher porosity (75 to 83%) than PI (60 to 73%) and PSF (70 to

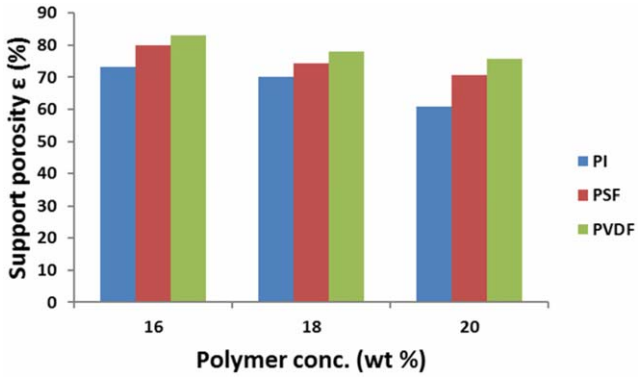

Figure 4. Bulk porosity of supports as a function of polymer type and polymer concentration in the casting solution. [Color figure can be viewed in the online issue, which is available at wileyonlinelibrary.com.]

80%) membranes, but differences are again rather small. As anticipated, porosities decreased as the concentration of polymer increased, resulting in somewhat less porous structures of the supports.[43–46,49]

Support Surface Morphology. Figure 5 presents the SEM surface micrographs of PSF [Figure 5(a–c)], PVDF (Figure 5(d–f)] and PI [Figure 5(g–i)] supports. As expected, the porosity of the supports decreased with increasing polymer concentration from 16 wt % to 20 wt % in the casting solution.

Morphology of the Support Cross-Sections. As expected, all supports had an asymmetric structure with a thin denser active layer over a thick more open sub-layer. It was observed that the surface pore morphology and the support bulk porosities (section 4.1.2) changed somewhat over the different chemistries and casting solution concentrations. SEM cross sections confirmed this trend, but also revealed important changes in morphology. SEM pictures of all these PSF supports showed the presence of macrovoids [Figure 6(a–c)]. In the case of PVDF supports [Figure 6(d–f)], similar macrovoids were observed for 16 wt % and 18 wt % polymer concentrations in the casting solution, but a clearly less open structure was observed for 20 wt %. Each time, a quite thick spongy substructure appeared at the bottom of the support layer in contrast with the non-woven. In PI supports, a membrane cast from a polymer concentration of 16% showed elongated macrovoids, but for 18 wt % and 20 wt %, a spongy structure appeared [Figure 6(g–i)]. An, increased polymer concentration in the casting solution results in a higher polymer concentration at the polymer/nonsolvent interface prior to the immersion in the nonsolvent coagulation bath. Therefore,

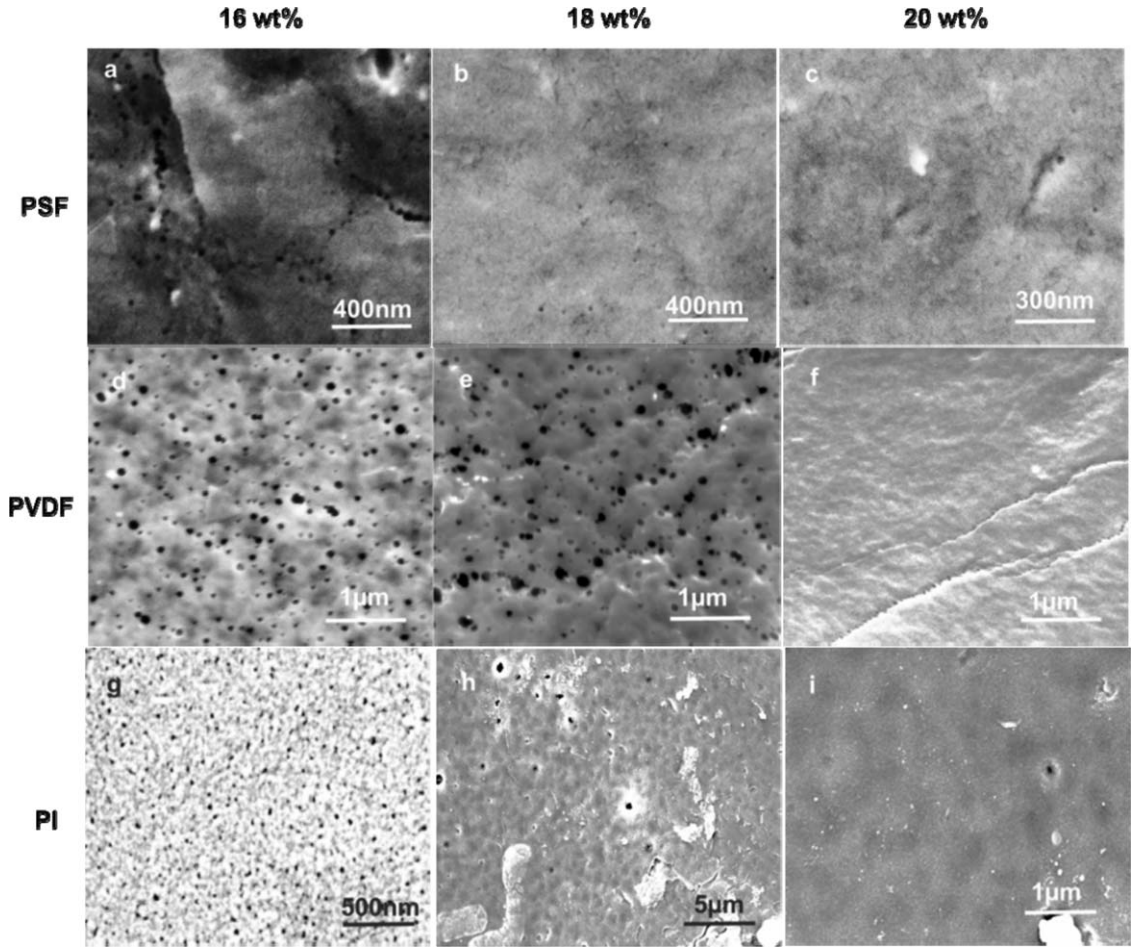

Figure 5. SEM surface micrographs of support membranes (top: PSF, middle: PVDF, and bottom: PI; with from left to right: 16 wt %, 18 wt %, and 20 wt % polymer concentration in the casting solution, respectively).

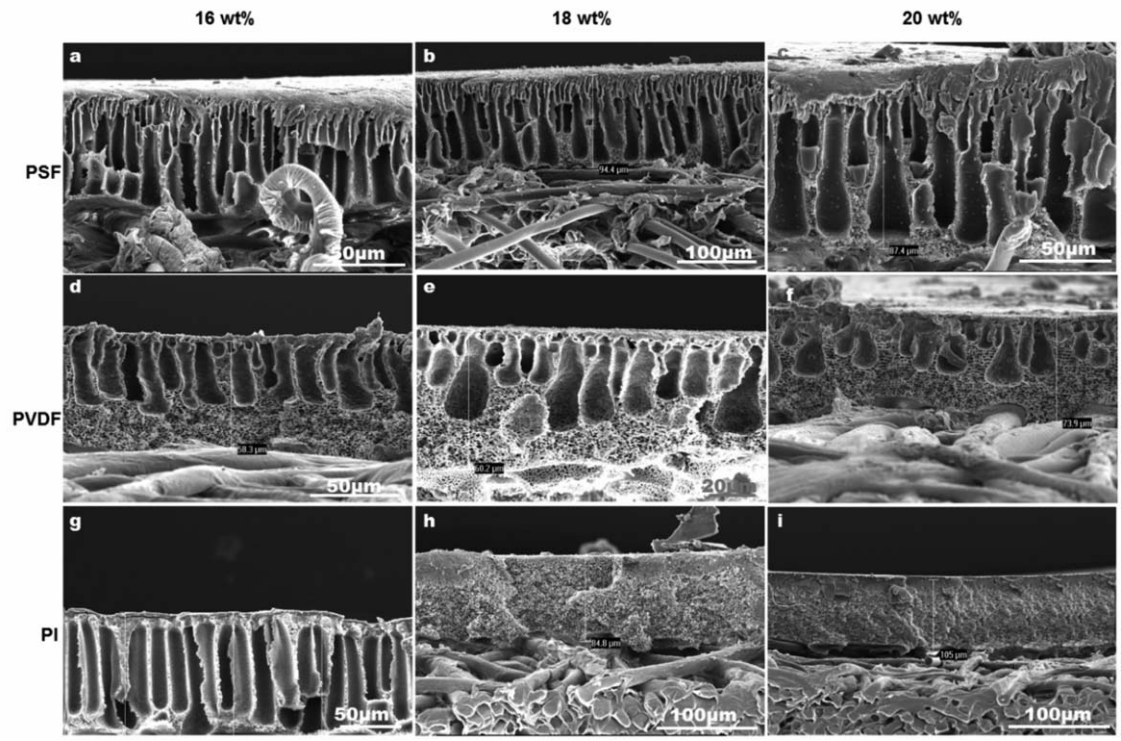

Figure 6. SEM cross-sectional micrographs of composite membranes (a to c: PDMS/PSF, d to f: PDMS/PVDF, and g to i: PDMS/PI, with from left to right 16 wt %, 18 wt %, 20 wt % polymer concentration in the casting solution, respectively).

diffusion of solvent and nonsolvent is slowed down, demixing is being delayed, leading to a decrease in the mean pore size, and surface porosity of the supports which imparts a spongy structure to the membrane.[43,44]

In general, the relatively high porosity of the support layer is expected to ensure a negligible resistance for the composite membrane during the pervaporation, even though the exact structure of the denser skin-layer cannot be visualized with SEM.

Support Thickness. Although the wet casting thickness was similar for all membranes (250 μm), the dry thicknesses differed significantly, ranging from PI (65–105 μm) to PSf (85–99 μm), and PVDF (28–45 μm). During phase inversion, polymer films always shrink significantly, since, on coagulation, solvent diffuses out of the polymer film, and the polymer solidifies, which lowers the volume and thus the thickness of the film.[55] This shrinkage obviously depends strongly on the polymer type.

Viscosity of the PDMS Coating Solutions

Figure 7 shows the changes in viscosity as a function of the crosslinking reaction time for three PDMS solutions with different concentrations. For a 20 wt % PDMS solution, the viscosity reaches 10 [mPa s] after 2 h, which is sufficient for applying a good coating layer. After 3 h, viscosity already jumped to almost 100 [mPa s] which made the solution too viscous to apply good coatings from. For a 10 wt % PDMS solution, it took almost 3 h to reach a viscosity value of 10 [mPa.s]. For the 5 wt % PDMS solution, no significant increase in viscosity could be observed at all, not even after 5 h. Due to its less critical changes in viscosity in short time intervals, the 10 wt % PDMS solution with 3 h cross-linking time was selected for subsequent coatings.

Gas Permeation Measurements

Total PDMS thickness (top layer + thickness of intruded PDMS in the pores of the support layer) of the composite membranes was determined from CO_2 gas permeation tests and compared with thickness determined by the SEM. However, the measurements were found unreliable for some membranes due to their overly thin PDMS layer which showed high permeation fluxes. The selected results are summarized in the Table II.

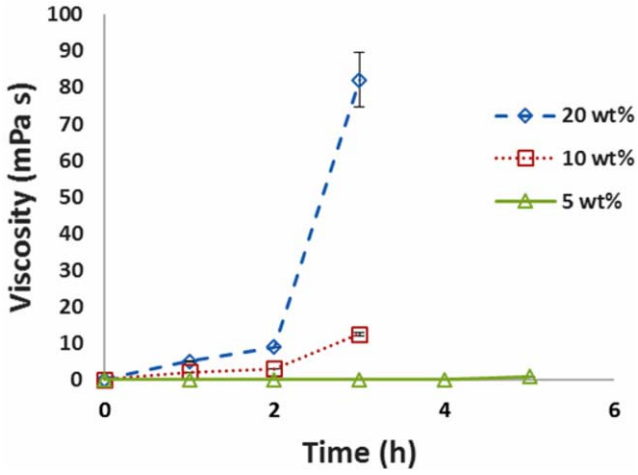

Figure 7. Crosslinking time vs. viscosity for PDMS solutions at 60 °C with three different concentrations in hexane. [Color figure can be viewed in the online issue, which is available at wileyonlinelibrary.com.]

Table II. Determination of Thickness of the PDMS Layer in the Composite Membranes

Support material	Concentration of polymer in support (wt %)	Dip time (min)	Thickness of the PDMS layer determined by	
			SEM	CO_2 permeation
PSF	16	2	1.2	1.6
	18		1.5	1.7
PVDF	16	4	1.3	1.5
	18		1.4	1.6
PI	16	2	1.3	1.8

Total PDMS thickness was significantly higher than the thickness visualized by scanning electron microcopy (SEM) for the membranes prepared with supports having a low polymer concentration (16 wt % and 18 wt %) in the casting solution.

It thus seems there is formation of a PDMS layer inside the support due to intrusion of PDMS solution during the dip coating or drying process. This resulted in an additional PDMS thickness which influences the overall pervaporation performance of the composite membrane as this layer is sterically confined and can thus swell less than the PDMS coated on top which is free to expand more.

Pervaporation

Influence of Support Polymer Type. The pervaporation fluxes of the composite membranes on the nine different supports reported above, can be arranged in the order PI >PVDF > PSF, while ethanol selectivity follows the order PSF > PVDF > PI (Figures 8–10). This trend can be explained as follows.

Support Pore Structure and Morphology. Depending on the pore size of the supports, various kinds of flows are possible. In the large pores, viscous flow of the permeating vapors occurs and the support does not interfere with mass transport. However, if the pores are small enough, the local vapor pressure can exceed the critical condensation pressure due to excessive resistance in the support towards removal of vaporized molecules by the vacuum pump, as commonly applied at lab-scale, resulting in capillary condensation. This capillary condensation reduces membrane performance by decreasing the driving force for pervaporation.[16] Hence, to avoid additional mass transfer resistance against the permeating compounds, the porosity of the supports should be high enough.[12]

The SEM images in Figure 5 revealed that an increasing polymer concentration in the casting solution decreased the surface pore size. It even changed the pore morphology in cross-sections (Figure 6) from finger-like to sponge-like for PI. This change in support structure affected the composite membrane performance as well (Figures 8–10). It can be seen that both flux and selectivity of the composite membranes decreased for supports cast from 18 wt % and 20 wt % polymer concentration. In the case of PI, the mass transfer resistance is more pronounced than for PSF and PVDF, consisting with the transition of a macrovoid structure to a spongy one. This would thus indicate, at least for the polymer and support structures studied here, that macrovoid-containing support layers would be most preferred.

Support Hydrophobicity/Hydrophilicity. From the contact angle values, the supports can be arranged in the order PVDF (95°) > PSF (81°) > PI (63°), as anticipated. It is striking in Figures 8–10 that PI-supports generally lead to lower membrane selectivities. It can thus be assumed that the better interaction of PI with water results in an increased water content in the permeate. More hydrophobic support materials thus seem more favorable for ethanol/water separations.

Influence of Polymer Concentration in the Support Casting Solution. Fluxes of the composite and unsupported membranes were normalized to a thickness of 10 μm for the selective layer. Even though the error on the PDMS-layer thickness determination could be significant (see for instance Figure 14). All normalized fluxes of the composite membranes are much lower than the one of the unsupported reference membrane. This could be due to a variety of factors, such as too limited support (surface) porosity (discussed in the sections 4.1.3 and 4.1.4), intrusion of the PDMS-layer in the support, or simply reduced swelling possibilities of the PDMS-layer when adhered to the support (discussed in the section 4.3.3).

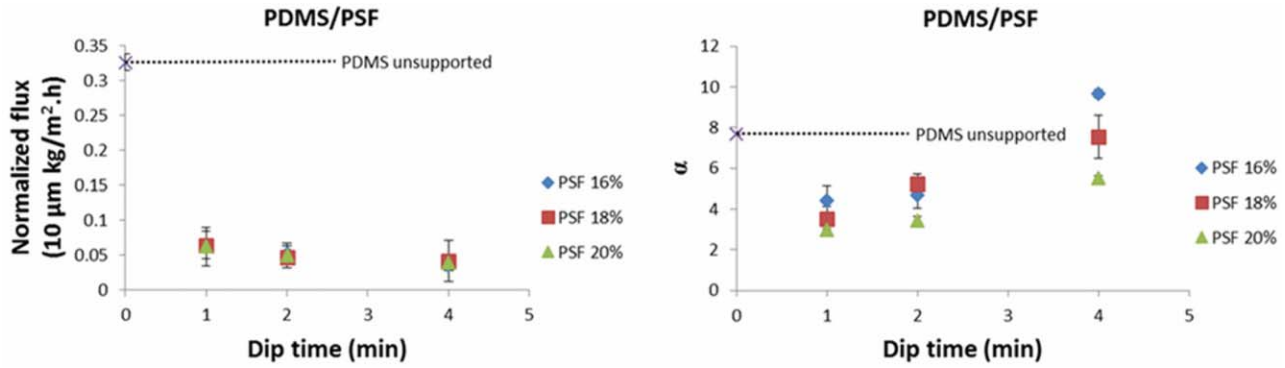

Figure 8. Effect of PSF concentration in the support casting solution and of dip time in the PDMS (10%) solution on the PV performance of PDMS–PSF membranes (left: flux normalized to a thickness of 10 μm; right: enrichment factor). [Color figure can be viewed in the online issue, which is available at wileyonlinelibrary.com.]

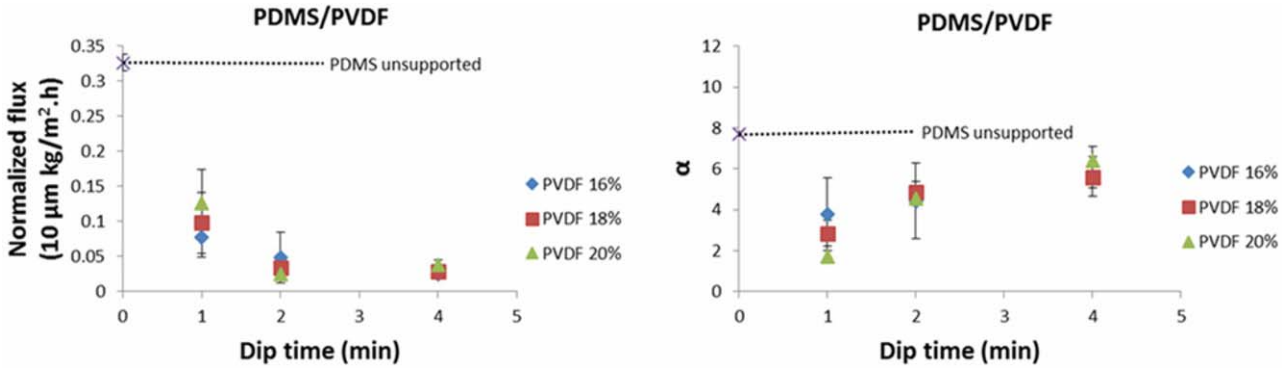

Figure 9. Effect of PVDF concentration in the support casting solution and of dip time in the PDMS (10%) solution on the PV performance of PDMS–PVDF membranes (left: flux normalized to a thickness of 10 µm; right: enrichment factor). [Color figure can be viewed in the online issue, which is available at wileyonlinelibrary.com.]

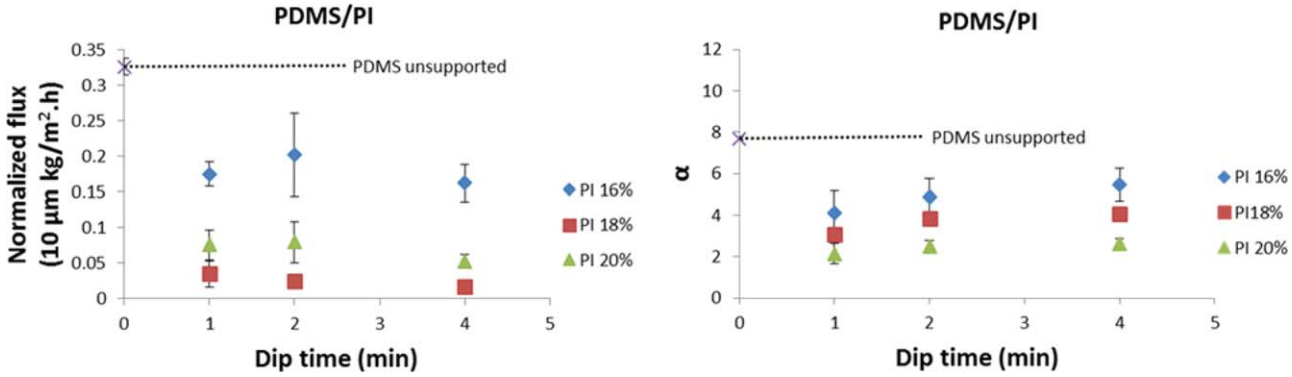

Figure 10. Effect of PI concentration in the support casting solution and of dip time in the PDMS (10%) solution on the PV performance of PDMS–PI membranes (left: flux normalized to a thickness of 10 µm; right: enrichment factor). [Color figure can be viewed in the online issue, which is available at wileyonlinelibrary.com.]

PSF Support. The PV performances of the PSF-supported composite PDMS-membranes is shown in Figure 8. Normalized fluxes were obtained in the range of 0.064 to 0.035 kg/m^{2}h and selectivities were in the range of 3 to 9.6. The highest selectivity of 9.6 was obtained when using a support cast from a 16 wt % PSF solution using a dip time of 4 min. This high selectivity is

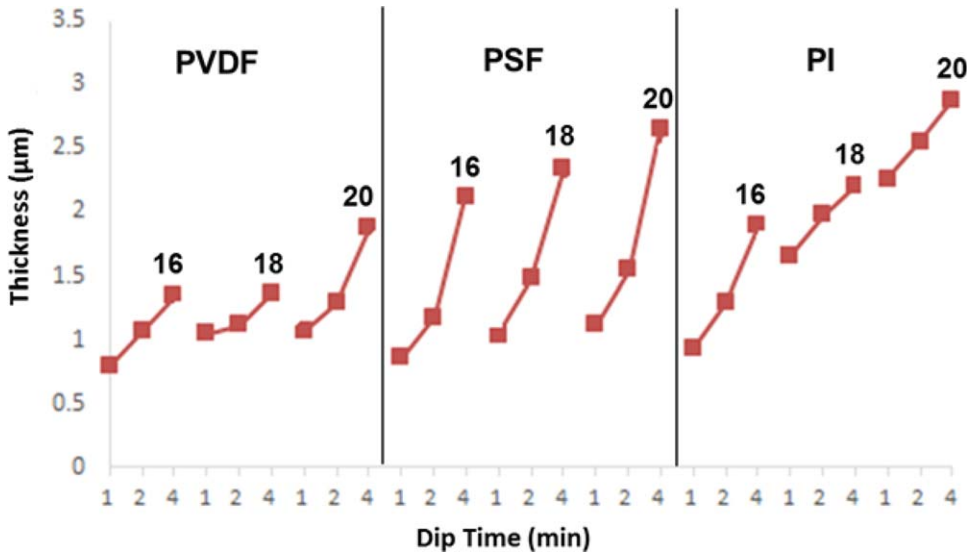

Figure 11. Thickness of the PDMS top layer as a function of dip time on the different types of supports (three different supports cast from three different casting solution concentrations: 16 wt %, 18 wt %, and 20 wt %). [Color figure can be viewed in the online issue, which is available at wileyonlinelibrary.com.]

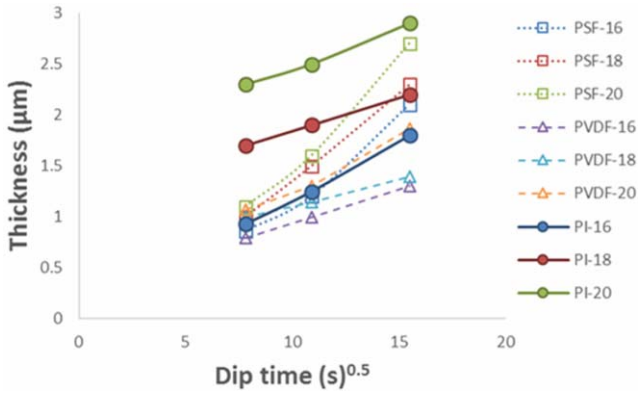

Figure 12. Thickness of the PDMS top layer as a function of the square root of dip time of the different types of supports (3 different supports cast from three different casting solution concentrations: 16 wt %, 18 wt %, and 20 wt %) in the PDMS solution (10 wt % PDMS in hexane, 3 h pre-crosslinked at 60 °C) at a constant withdrawal speed of 0.01 m/s. [Color figure can be viewed in the online issue, which is available at wileyonlinelibrary.com.]

unfortunately combined with a rather low normalized flux of 0.036 kg/m^{2}h. Composite membranes with supports prepared from 18 wt % and 20 wt % PSF-solutions showed reduced selectivities probably due to the decreased porosities of the supports.

PVDF Support. The PV performances of the PVDF supported PDMS composite membranes is shown in Figure 9. Normalized fluxes were in the range of 0.12 to 0.03 kg/m^{2}h and selectivities varied from 1.7 to 6.4. The fluxes were generally higher than for the PDMS/PSF composite membranes, probably due to the more hydrophobic character in combination with the more open pore structure of the PVDF support which can be linked to the higher pure water fluxes. A maximum selectivity of 6.4 was obtained for a 20 wt % PVDF concentration and a dip time of 4 min.

PI Support. The PV performances of the composite PDMS/PI membranes is shown in Figure 10. Normalized fluxes of the membranes were in the range of 0.2 to 0.02 kg/m^{2}h and selectivities varied from 2.1 to 5.5. The maximum selectivity value of 5.5 was obtained for PI 16 wt % with a dip time of 4 min. Higher fluxes but lower selectivities were generally observed compared to the above described composite membranes which might be due to the hydrophilic nature of PI.

Influence of the Dip Time of the Supports in the PDMS Solution. The change in dip time of the supports in the PDMS solution was studied to form more uniform, defect-free layers. Figure 11 shows the thickness of the PDMS top-layer as a function of dip time on the different types of supports.

It can be seen that the thickness of the PDMS layer clearly increases with increasing polymer concentration in the casting solution of the support and with increasing dip time. The first effect can most probably be related to intrusion of the PDMS solution in support, which will decrease systematically with increasing polymer concentration, since support porosities and surface pore sizes tend to decrease. Babaluo *et al.* developed a model to predict the effects of variable dip time and withdrawal speed of porous supports on the thickness of the top layer.[56] According to the model, for a fixed combination of coating solution and porous support, the top layer thickness increases linearly with the square root of the dip time ($t^{0.5}$) at a constant withdrawal speed of the support. Figure 12 shows the thickness of the PDMS top-layer as a function of the square root of the dip time for the different types of supports.

It can be seen that, all lines in the Figure 12 are in accordance with the model. The increase in the thickness of the PDMS layer as a function of dip time, that is, the slope of the lines, follows the order of PSF $\gg$ PVDF > PI. The Hildebrand-parameters of the different polymers utilized in this work are listed below:

1. PDMS 14.9 (Mpa^1/2)
2. PSF 20.2 (Mpa^1/2)
3. PVDF 23.2 (Mpa^1/2)
4. PI 24.3 (Mpa^1/2)

Considering the Hildebrand-parameters of the different polymers, it is clear that this order follows the order of decreasing interactions between the support material and PDMS. A better chemical interaction with the support thus leads to enhanced

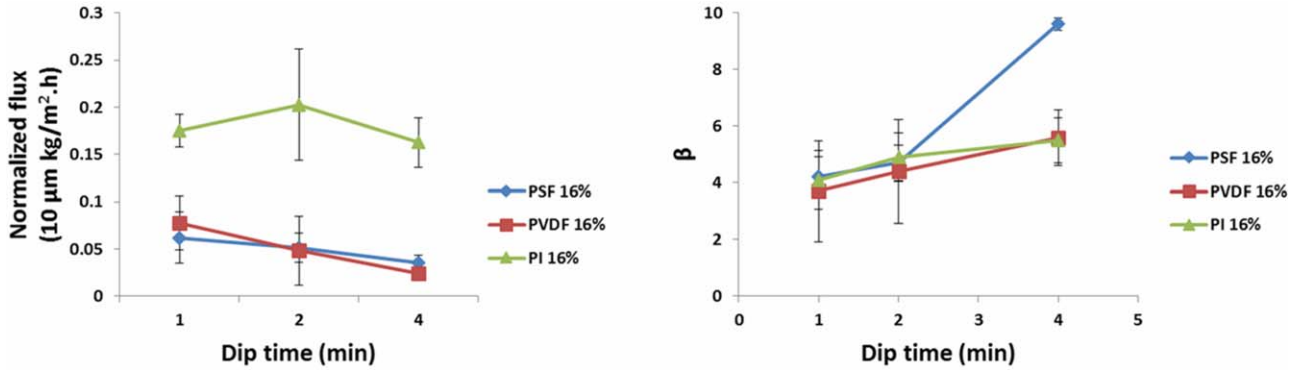

Figure 13. Effect of dip time on the performance in PV for PDMS composite membranes prepared on PSF, PVDF and PI supports, cast from their 16 wt % casting solutions (left: normalized flux; right: enrichment factor). [Color figure can be viewed in the online issue, which is available at wileyonlinelibrary.com.]

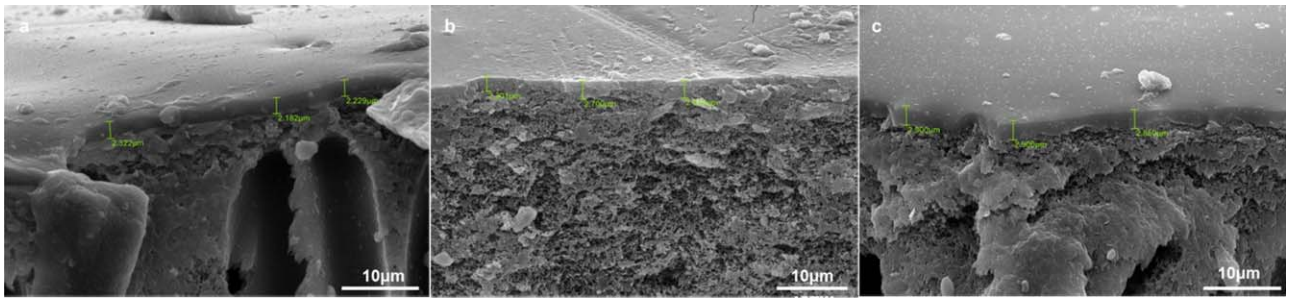

Figure 14. SEM cross section micrographs of PDMS/PI (20 wt % casting solution) composite membranes showing the effect of increasing dip time (*a*= 1 min, *b*= 2 min, *c*= 4 min). [Color figure can be viewed in the online issue, which is available at wileyonlinelibrary.com.]

adsorption of polymer chains from the coating solution during the dip time, and hence the deposition of a thicker PDMS-layer.

It is clear from Figure 13 that the selectivities of the composite membranes increased with increasing dip time, while the fluxes declined gradually, due to an increased thickness of the PDMS selective layer. These thickness values were derived from SEM images, as typically presented in Figure 14. Thus, composite membranes prepared with increased dip time result in the uniform coating of defect-free PDMS solutions to create membranes with a good selectivity.

Comparison with Literature

The pervaporation performances of different PDMS supported membranes reported by other research groups for comparable ethanol-water mixture separations are listed in Table III. The composite PDMS membranes prepared in this work on different supports and with PDMS top layer thicknesses varying from 0.79 μm to 2.8 μm, showed total fluxes from 20 to 200 g/m^2.h and selectivities from 1.7 to 9.6 for the separation of a 6 wt % aqueous ethanol solution at a feed temperature of 40 °C.

In comparison with the literature data, the selectivities and fluxes obtained in present work were not the highest, but a good comparable performance was obtained. It should be emphasized that proper comparison with literature is difficult as different preparation conditions are adopted by other research groups, for example, source and type of PDMS,[26] support casting conditions,[27] post-treatment on the support[17] coating conditions of the PDMS layer.[17,26–28] In addition, operational conditions during PV (e.g., feed concentration) can also substantially influence results.

CONCLUSIONS

Both flux and selectivity for PDMS coated PV membranes in the removal of ethanol from aqueous feeds are clearly influenced by the support layer. Three polymers with different chemical composition were used in this work to prepare support layers having comparable surface porosities to obtain the PDMS composite membranes. Resistance of the support layers increased by increasing the polymer concentration in the casting solutions of the supports. This could be attributed to a decreased pore size in the support, as indicated by SEM images, and a gradual decrease in pure water flux. For the current separation, a hydrophobic support material with macrovoid structure was found optimal. For the composite membranes, a certain pre-crosslinking time of the dilute PDMS coating solution prior to dipping was found essential. Enhanced performance, especially in the selectivity of the composite membranes, was realized by increasing the dip time in the PDMS coating solution. SEM analysis of the composite membranes showed that this leads to a minor increase in the thickness

Table III. PV Performance of the PDMS Coated Composite Membranes for the Separation of 6 wt % Ethanol/Water Mixture (All Measured at 40 °C)

Support	Thickness of PDMS layer (μm)	Feed concentration (wt %)	Flux normalized to 10 μm (g/m^{2}h)	Separation factor (α)	PSI	Reference
PSF	6	5	600-4000	1.79-5.2	2.5-3.2	27
PSF	1	2-5	160	5	0.64	28
PVDF	10	5	500	8.3	3.6	26
Crosslinked PI	12.5	3-9	120-130	4.6	0.47	17
PSA/PA[a]	5	2-5	300	11	3	28
PSF	0.86 to 2.65	6	64-35	3-9.6	0.13-0.3	This study
PVDF	0.79 to 1.87	6	120-30	1.7-6.4	0.08-0.2	This study
PI	0.93 to 2.88	6	200-20	2.1-5.5	0.22-0.1	This study
PDMS unsupported	120	6	320	7.7	2.1	This study

[a] PSA/PA- Polysulfonamide blend with polyamide.

of the PDMS top layer. For a certain PDMS coating solution and porous support, the top layer thickness increased linearly with the square root of the dip time ($t^{0.5}$) at a constant withdrawal speed of the support. Single gas permeation tests proved the intrusion of PDMS solution inside the pores of the support. This resulted in an additional PDMS thickness which increased the overall pervaporation selectivity of the composite membranes.

ACKNOWLEDGMENTS

The authors gratefully acknowledge Belgian Government (IAP-PAI networking), the Flemish Government (Methusalem (CASAS) and FWO (G069811) and KU Leuven (IOFKP/10/002 and OT 11/061 projects) for the financial support.

REFERENCES

1. Lin, Y.; Tanaka, S. *Appl. Microbiol. Biotechnol.* **2006**, *69*, 627.
2. Hoogwijk, M.; Faaij, A.; Broek, R.; Berndes, G.; Gielen, D.; Turkenburg, W. *Biomass. Bioenerg.* **2003**, *25*, 119.
3. Lynd, L. R.; Cushman, J. H.; Nichols, R. J.; Wyman, C. E. *Science* **1991**, *251*, 1318.
4. Vane, L. M. *Biofuels Bioprod. Bioref.* **2008**, *2*, 553.
5. Cysewski, G. R.; Wilke, C. R. *Biotechnol. Bioeng.* **1977**, *19*, 1125.
6. Kollerup, F.; Daugulis, A. J. *Can. J. Chem. Eng.* **1986**, *64*, 598.
7. Oulman, C. S, Chriswell, C. D. U.S. Pat 4,277,635 **1981**.
8. Shabtai, Y.; Chaimovitz, S.; Freeman, A.; Katchalski-Katzir, E.; Linder, C.; Nemas, M.; Perry, M.; Kedem, O. *Biotechnol. Bioeng.* **1991**, *38*, 869.
9. Ulutan, S.; Nakagawa, T. *J. Membr. Sci.* **1998**, *143*, 275.
10. Chovau, S.; Gaykawad, S.; Straathof, A. J. J.; Van der Bruggen, B. *Bioresour. Technol.* **2011**, *102*, 1669.
11. O'Brien, D. J.; Craig, J. C. *Appl. Microbiol. Biotechnol.* **1996**, *44*, 699.
12. Ping, P.; Baoli, S.; Yongqiang, L. *Sep. Sci. Technol.* **2011**, *46*, 234.
13. Gudernatsch, W.; Menzel, T.; Strathmann, H. *J. Membr. Sci.* **1991**, *61*, 19.
14. Lipnizki, F.; Olsson, J.; Wu, P.; Weis, A.; Tragardh, G.; Field, R. W. *Sep. Sci. Technol.* **2002**, *37*, 1747.
15. Claes, S.; Vandezande, P.; Mullens, S.; Leysen, R.; De Sitter, K.; Andersson, A.; Maurer, F. H. J.; Van den Rul, H.; Peeters, R.; Van Bael, M. K. *J. Membr. Sci.* **2010**, *351*, 160.
16. Trifunovic, O.; Tragardh, G. *J. Membr. Sci.* **2005**, *259*, 122.
17. Dobrak, A.; Figoli, A.; Chovau, S.; Galiano, F.; Simone, S.; Vankelecom, I. F. J.; Drioli, E.; Van der Bruggen, B. *J. Colloid Interface Sci.* **2010**, *346*, 254.
18. Nijhuis, H. H.; Mulder, M. H. V.; Smolders, C. A. *J. Membr. Sci.* **1991**, *61*, 99.
19. Heintz, A.; Stephan, W. *J. Membr. Sci.* **1994**, *89*, 153.
20. Bai, J.; Fouda, A. E.; Matsuura, T.; Hazlett, J. D. *J. Appl. Polym. Sci.* **1993**, *48*, 999.
21. Rautenbach, R.; Helmus, F. P. *J. Membr. Sci.* **1994**, *87*, 171.
22. Bode, E.; Hoempler, C. *J. Membr. Sci.* **1996**, *113*, 43.
23. Liu, M. G.; Dickson, J. M.; Cote, P. *J. Membr. Sci.* **1996**, *111*, 227.
24. Smart, J.; Schucker, R. C.; R. Lloyd, D. *J. Membr. Sci.* **1998**, *143*, 137.
25. Vankelecom, I. F. J.; Moermans, B.; Verschueren, G.; Jacobs, P. A. *J. Membr. Sci.* **1999**, *158*, 289.
26. Han, X.; Wang, L.; Li, J.; Zhan, X.; Chen, J.; Yang, J. *J. Appl. Polym. Sci.* **2011**, *119*, 3413.
27. Tan, S.; Li, L.; Zhang, Z.; Wang, Z. *Chem. Eng. J.* **2010**, *157*, 304.
28. Shi, E.; Huang, W.; Xiao, Z.; Li, D.; Tang, M. *J. Appl. Polym.* **2007**, *104*, 2468.
29. Gevers, L. E. M.; Aldea, S.; Vankelecom, I. F. J.; Jacobs, P. A. *J. Membr. Sci.* **2006**, *281*, 741.
30. Claes, S.; Vandezande, P.; Mullens, S.; Sitter, K. D.; Peeters, R.; Van Bael, M. K. *J Membr. Sci.* **2012**, *389*, 265.
31. Wei, W.; Xia, S.; Liu, G.; Dong, X.; Jin, W.; Xu, N. *J. Membr. Sci.* **2011**, *375*, 334.
32. Liu, G.; Xiangli, F.; Wei, W.; Liu, S.; Jin, W. *Chem. Eng. J.* **2011**, *174*, 495.
33. Xiangli, F.; Chen, Y.; Jin, W.; Xu, N. *Ind. Eng. Chem. Res.* **2007**, *46*, 2224.
34. Kim, I. C.; Yun, H. G.; Lee, K. H. *J Membr. Sci.* **2002**, *199*, 75.
35. Stafie, N.; Stamatialis, D. F.; Wessling, M. *J. Membr. Sci.* **2004**, *228*, 103.
36. Stafie, N. Ph.D. thesis, University of Twente, Enschede, The Netherlands, **2004**.
37. Stafie, N.; Stamatialis, D. F.; Wessling, M. *Sep. Purif. Technol.* **2005**, *45*, 220.
38. Wang, R.; Shan, L.; Zang, G.; Ji, S. *J. Membr. Sci.* **2013**, *432*, 33.
39. Zhu, J.; Fan, Y.; Xu, N. *J. Membr. Sci.* **2011**, *367*, 14.
40. Peng, F.; Liu, J.; Li, J. *J. Membr. Sci.* **2003**, *222*, 225.
41. Madaeni, S. S.; Mohammadi Sarab Badieh, M.; Vatanpour, V. *Polym. Eng. Sci.* **2013**, *53*, 1878.
42. Qtaishata, M.; Khayet, M.; Matsuura, T. *J. Membr. Sci.* **2009**, *341*, 139.
43. Holda, A. K.; Aernouts, B.; Saeys, W.; Vankelecom, I. F. J. *J. Membr. Sci.* **2013**, *442*, 196.
44. Holda, A. K.; Vankelecom, I. F. J. *J. Appl. Polym. Sci.* **2015**, *132*, 42130.
45. Vandezande, P.; Gevers, L. E. M.; Jacobs, P. A.; Vankelecom, I. F. J. *Sep. Purif. Technol.* **2009**, *66*, 104.
46. Vandezande, P.; Li, X.; Gevers, L. E. M.; Vankelecom, I. F. J. *J. Membr. Sci.* **2009**, *330*, 307.
47. Bottino, A.; Camera-Rodab, G.; Capannelli, G.; Munari, S. *J. Membr. Sci.* **1991**, *57*, l.
48. Liu, F.; Hashim, N. A.; Liu, Y.; Moghareh Abed, M. R.; Li, K. *J. Membr. Sci.* **2011**, *375*, 1.
49. Lia, Q.; Xua, Z. L.; Liub, M. *Polym. Adv. Technol.* **2011**, *22*, 520.

50. Available at: http://www.solvayplastics.com/sites/solvayplastics/EN/specialty_polymers/Markets/Membranes/Pages/sulfone-polymers-membranes.aspx
51. Available at: http://catalog.ides.com/Datasheet.aspx?I=92041&U=0&FMT=PDF&E=111432
52. Available at: http://polymer-additives.specialchem.com/product/a-huntsman-matrimid-9725
53. Available at: http://www.html-membrane.be
54. Available at: http://www.emdmillipore.com/US/en/product/Stirred-Cell-Model-8050%2C-50%C2%A0mL,MM_NF-5122
55. Hendrix, K.; Koeckelberghs, G.; Vankelecom, I. F. J. *J. Membr. Sci.* **2014**, *452*, 241.
56. Babaluo, A. A.; Kokabi, M.; Manteghian, M.; Sarraf-Mamoory, R. *J. Eur. Ceram. Soc.* **2004**, *24*, 3779.